Joint Hurricane Testbed Year 1 Report
August 1, 2010 to July 31, 2011

Improvement in the rapid intensity index by incorporation of inner-core information

Principle Investigator: John Kaplan
Hurricane Research Division
NOAA/AOML

Co-PIs: Joe Cione(NOAA/HRD), Mark DeMaria(NOAA/NESDIS), Jack Dostalek (CIRA), Jason Dunion (CIMAS/HRD), John Knaff (NOAA/NESDIS), Jun Zhang (CIMAS/HRD)

Co-Investigators: Thomas Lee (NRL) and Jeff Hawkins (NRL)

Scientific/ computer scientist support: Evan Kalina (FSU) and Paul Leighton (NOAA/HRD)

NHC Points of contact: Lixion Avila, Eric Blake, Todd Kimberlain, Chris Sisko, and Chris Landsea

1. Background

The overall goal of this JHT funded project was to improve the existing operational SHIPS rapid intensification index (RII) described in Kaplan et al. (2010) by incorporating predictors from three new sources of information: GOES infra-red (IR) imagery, total precipitable water (TPW) derived from microwave SSM/I imagery, and boundary-layer predictors derived from GFS analyses. Although the proposal called for improvements to both the Atlantic and East Pacific version of the operational RII, the first year of the project was designed to focus primarily on the development and testing of the new RI predictors for the Atlantic basin version of the RII while the second year was designed to do the same for the East Pacific version.

2. Development of new Atlantic RI predictors

a. Time evolution of GOES IR imagery

The CIRA Tropical cyclone IR image archive was updated to include more imagery from the 1995 Atlantic hurricane season. Complete storm histories were added for Allison, Barry, Gabrielle, TD14, Noel, Pablo Sebastien, and Tanya and the imagery histories for Humberto, Iris, Jerry, Karen, Luis, Marilyn, Opal, and Roxanne were improved. The updated image archive was then employed to perform Empirical Orthogonal Function/Principle Component Analysis on the storm relative, motion rotated imagery. Using the first 9 EOFs, predictors for the SHIPS database were then generated for testing with respect to rapid intensification (RI). These included the six-hour averages of the first nine EOFs and their standard deviations as well as the regression coefficients associated with these six-hour periods.

b. Total Precipitable water

The total precipitable water (TPW) derived using SSM/I TMI and AMSR-E imagery every 6 hours for the period from 1995-2008 for the region from 0-60° N and 0-100° W that was supplied by NRL was employed to compute several storm relative TPW predictors. These predictors included the total precipitable water (TPW) azimuthally averaged from r=0 to r=100 km, the TPW azimuthally averaged from r=100 to r=200 km, %TPW less than 45 mm in radii r=0 to r=200 km and r=400 to r=600 km in the N, W, S and E quadrants, the %TPW less than 45 mm, r=0 to r= 200 km and r=400 to r=600 km, front, left, back, right quadrants (storm motion relative quadrants), the %TPW less than 45 mm, r=0 to r=500 km, 90° quadrant centered upshear, TPW averaged r=0 to r=500 km, 90° quadrant centered upshear, and TPW averaged r=0 to r=500 km. The above TPW predictors were then added to the SHIPS database so that they could be subjected to testing for potential inclusion in the new experimental RII. In addition, software was written to read the HDF4 TPW files generated by NESDIS/OSDPD and then convert them to a simple ASCII-formatted lat./lon. grid for future processing. Finally, the routines required to read this file format were created.

c. Boundary-layer predictors:

Atmospheric temperature and moisture data obtained from the NCEP GFS analyses and sea-surface temperature (SST) estimates derived from the Reynolds gridded SST analysis and an inner-core cooling algorithm (Cione et al. 2007) were used to compute air-sea temperature and moisture differences and to estimate surface sensible and latent heat fluxes within the storm's inner-core region. A total of fifteen such boundary-layer predictors were computed directly from the GFS data and added to the SHIPS database for the Atlantic basin. An additional thirty-five Atlantic basin boundary-layer predictors were also computed by applying empirical relationships that were previously developed from buoy data (Cione and Uhlhorn 2003, Cione et. al. 2005) to the GFS and SST fields.

3. Derivation of experimental Atlantic RII

a. Selection of predictors

As a first step at screening the above predictors for their ability to increase the skill of the operational RII, each was subjected to statistical significance testing for a homogenous sample of Atlantic cases for the 1995-2008 sample. Those predictors whose mean values for the developmental RI and non-RI samples were shown to be statistically different (at $\geq$ 99.9% level based upon a standard 2-sided t-test) were tested for their ability to increase the skill of the operational RII. This was accomplished by substituting the statistically significant predictors for select predictors in the existing operational RI shown in Table 1. Specifically, the new TPW predictors were tested as replacement to the 850-700 mb relative humidity (RH) predictor since both are measures of atmospheric moisture, while the GOES-IR PC predictors were tested as replacement for the two existing inner-core GOES predictors since they are all measures of inner-core organization as deduced using GOES IR imagery. Finally, the new GFS boundary-layers predictors were tested in place of the potential intensity and ocean heat content predictors since each of these is related to boundary-layer processes.

Sensitivity tests were then performed to determine if any of the new predictors increased the skill of the RII when they were substituted for predictors in the existing operational version that is listed in Table 1. The change in skill of each of the new predictors was then assessed by comparing the average skill of the experimental RII to that obtained using the current operational predictors using the methodology described in Kaplan et al. 2010 for the three RI thresholds that are used in the current operational RII (25-kt, 30-kt, and 35kt) as well as an additional RI threshold of 40 kt for which a version of the RII was developed and tested at the request of one of our NHC points of contact (Eric Blake).

Previous 12-h intensity change
850-200 mb vertical shear from 0-500 km radius
200 mb divergence from 0-1000 km radius
850-700 mb relative humidity from 200-800 km radius
Percent area from 50-200 km covered by -30°C GOES-IR brightness temperatures
Std. dev of 50-200 km GOES-IR brightness temperatures
Potential intensity (Current intensity – maximum potential intensity)
Oceanic heat content

Table 1. Predictors used in the current operational Atlantic RII.

Based upon the above sensitivity tests, three new predictors were selected to replace those in the existing operational version. The first of these three new predictors is the percentage of the area within 500 km radius 90° upshear of the storm center with TPW < 45 mm at time T=0 h. This predictor is used as a replacement to the 850-700 mb RH in the new experimental version of the Atlantic RII. Rapid intensification is favored when this predictor is small and hence the amount of dry air that is being advected into the storm circulation is relatively small. The cutoff of 45 mm as a delineator for dry air is based upon the results of Dunion (2010). Figure 1 shows an example of the distribution of TPW around several storms during the 1995 season. The blue and green areas (TPW <45 mm) represent regions where the atmosphere is relatively dry between the surface and 500 mb (where 90-95% of the contribution from TPW comes from) while the orange and red areas (TPW > 45 mm) represent regions where the atmosphere is relatively moist.

Another one of the new RI predictors is the second principle component (PC2) computed from the GOES-IR imagery following the methods described in Knaff (2008). This predictor is used as a replacement for the percent area covered with GOES-IR brightness temperatures <-30° C in the new experimental version of the Atlantic RII. Figure 2 shows the favored overall pattern of the EOF for PC2 as well as an example of what the GOES-IR imagery looked like just prior to

Hurricane Wilma's period of RI during the 2005 Hurricane Season. The image shows that convection tends to be enhanced in the left front quadrant while being suppressed in the right rear quadrant near the time that RI commences. This pattern often precedes axisymmetrizaton of the IR imagery (Knaff 2008).

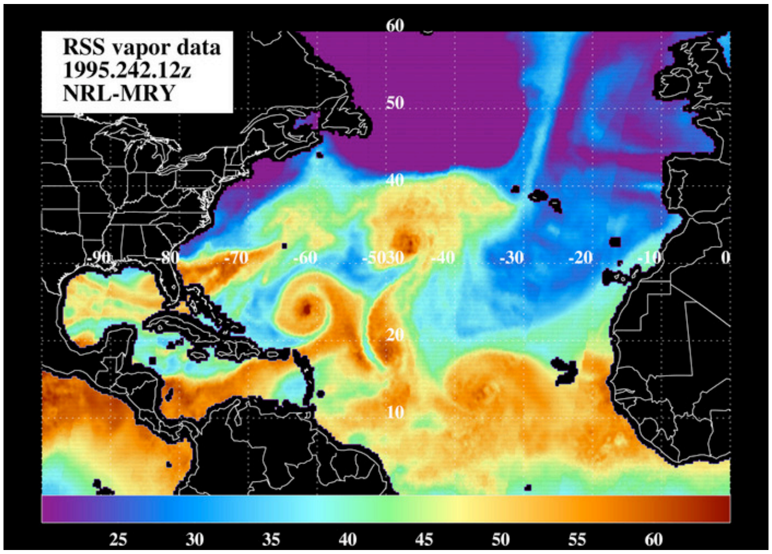

Fig. 1. Total precipitable water (TPW) during a select day during the 1995 season. Data provided courtesy of RSS and NRL-Monterey.

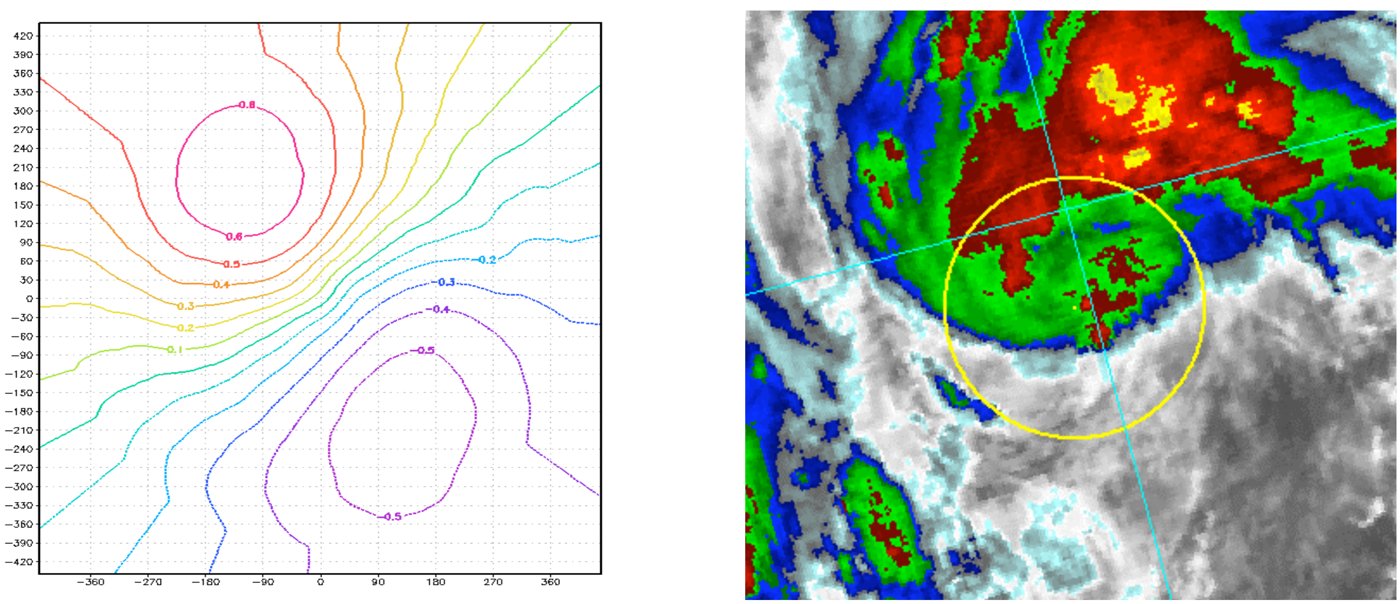

Fig. 2. Preferred pattern of PC2 (left) and an example of the corresponding GOES-IR representation for Hurricane Wilma at 1745 UTC on 17 October (right). The yellow circle denotes a circle with a radius of 440 km. The direction of motion is to the top center of both diagrams.

The last new predictor is the inner-core dry air predictor that is given by:

$$(q10_{layer} - q10)*Vmx \qquad 1$$

where q10 is the inner-core specific humidity at 10 m obtained using the GFS 1000 mb temperature and relative humidity (RH) between 200 and 800 km radius, $q10_{layer}$ is the 10 m specific humidity obtained using the ambient 200-800 km radius 1000 mb T and the layer-mean RH from 1000 mb to 500 mb, and Vmx is the NHC maximum sustained wind at t=0 h. The value of q10 is obtained by bringing the 1000 mb air down to the surface (dry adiabatically if unsaturated at 1000 mb and moist adiabatically if air is saturated) and then allowing the air to cool assuming that the RH reaches 95% as the parcel spirals into the storm core. The value of $q10_{layer}$ is obtained following the same methodology using the 1000 mb T but using the layer-mean RH between 1000 and 500 mb instead of using only the RH at 1000 mb. Although this predictor was tested in place of the potential intensity and ocean heat content predictors that are currently used in the operational RII, it was ultimately used as a replacement to ocean heat content since it increased the skill of the RII when substituted for this predictor but not when it was substituted for the potential intensity predictor. It is should be noted that small values of the inner-core dry air predictor, indicating less potential for dry air to mix down to the surface, are favored for RI.

In addition to replacing the three old operational RI predictors with three new ones described above, the scaling methodology that was used for the potential intensity and persistence predictors was modified slightly since sensitivity tests showed that doing so improved the overall skill of the model for the developmental sample. Thus, for the dependent sample about half of the increase in skill resulted from changes in the scaling methods that were used for these two predictors and half resulted from the use of the three replacement predictors. Table 2 shows the predictors used in the new experimental Atlantic RII.

Previous 12-h intensity change
850-200 mb vertical shear from 0-500 km radius
200 mb divergence from 0-1000 km radius
Total precipitable water
PC-2 from GOES-IR principle component analysis
Std. dev of 50-200 km IR brightness temperatures
Potential intensity (Current intensity – maximum potential intensity)
Inner-core dry air predictor

Table 2. Predictors used in the new experimental Atlantic RII.

Figure 3 shows the average relative weights of the RII predictors for all four RI thresholds (25-kt, 30-kt, 35-kt and 40-kt) that are determined from linear discriminant analysis (see Kaplan et al. 2010). The percentage of the weight of the three new RI predictors to the total of the weights of all eight RI predictors was also computed and then compared to that of three predictors that they replaced. These percentages were obtained by summing the weights of the three replacement (operational) RI predictors and then dividing those by the sum of the relative weights of all eight RI predictors that are used in the replacement (operational) RII. It can be seen that the new predictors represent about 23% of the total weight of the eight RI predictors while the old operational predictors are only about 12%.

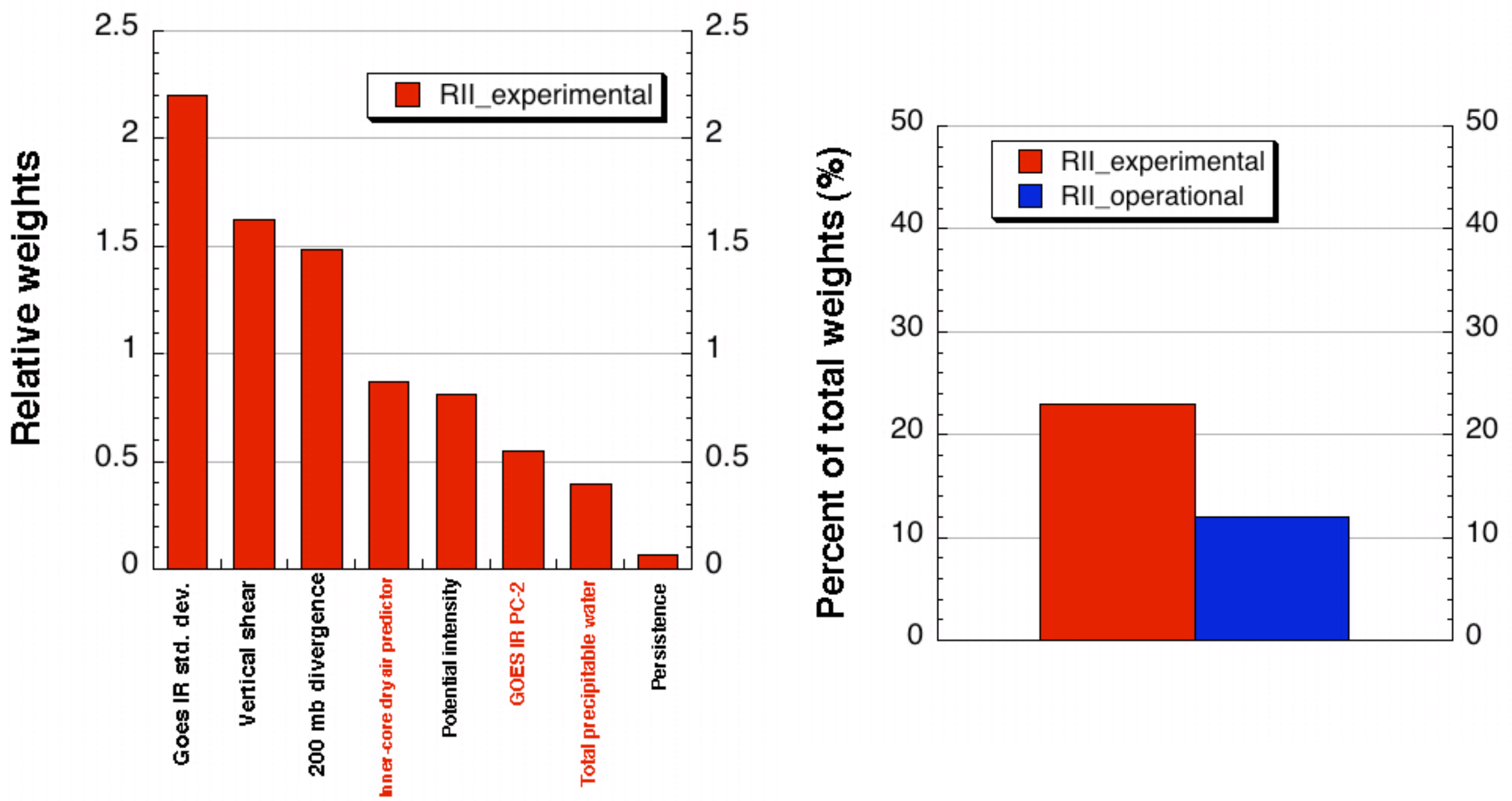

Fig 3. Average relative weights of the RI predictors for the 25-kt, 30-kt, 35-kt and 40-kt RI thresholds for the new Atlantic experimental RII (the new predictors are higlighted in red) for the 1995-2008 developmental sample (left panel) and percentage contribution of three new replacement (red) and corresponding replaced operational (blue) RI predictors to the sum of the weights of the eight RI predictors that are used in the new experimental and old operational RII.

The level of skill of the new experimental Atlantic RII index was compared to that of the current operational RII by performing a cross-validation for the 1995-2008 sample. To accomplish this, each of the 14 years that comprised the 1995-2008 sample were excluded one year at a time and the RII was re-derived and then re-run on cases from the excluded year. The results from each of the individual years were then combined to get the skill of each version of the RII for the total 14 year sample. Fig. 4 shows the skill of the RII for the 1995-2008 cross-validated sample. The figure indicates that the new experimental RII increases the mean absolute skill of the RII for each of the RI thresholds save for the 40 kt threshold. The slight degredation in skill found for that threshold may be due in part to the rather small sample size since there were only 64 RI cases for the entire 1995-2008 sample for the 40-kt threshold. Nevertheless, the average absolute skill of the new experimental RII was 3.1% higher than it was for the current operational version which represents roughly a 26% relative improvement in skill for the 4 RI thresholds studied. Moreover, the increase in skill of the new experimental RII for the 30-kt RI threshold was about 7% higher than the old operational version which represents a 60% relative increase in skill.

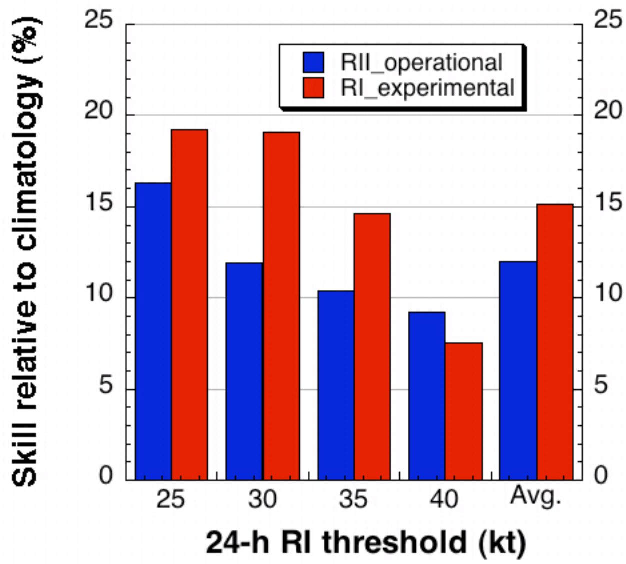

Fig. 4. Cross-validated skill of the current operational and new experimental RII for the 1995-2008 Atlantic sample. The skill for each individual threshold as well as the average skill (Avg.) for all 4 RI thresholds is shown.

Although ocean heat content is not employed as a predictor in the recently developed experimental version of the Atlantic RII, results obtained when re-deriving the operational RII for the 2010 Hurricane indicate that it may have the potential to provide additional skill particularly for the higher RI thresholds. As a test of this hypothesis, ocean heat content was added as a 9th predictor to the experimental Atlantic RII and the skill of this version was compared to that of the existing version for the 1995-2008 sample (Fig. 5). It can be seen that, on average, the addition of ocean heat content resulted in an increase in skill of the RII when tested on both the dependent and cross-validated 1995-2008 sample although a degradation in skill occurred for some of the indivdual RI thresholds for the cross-validated sample. In light of these results, ocean heat content will be tested as an additional predictor when the expermiental Atlantic RII is re-derived using the updated 1995-2009 developmental sample in preparation for real-time testing during the latter part of the upcoming 2010 Hurricane Season.

4. Preparation of Atlantic RII for real-time testing during the 2010 Hurricane Season

In preparation for testing of the experimental RII during the 2010 Hurricane Season, an offset correction was determined by comparing the NESDIS operational TPW product with the NRL TPW analyses that were used to derive the experimental Atlantic RII. This offset will be applied to the operational NESDIS TPW product that will be employed when running the experimental

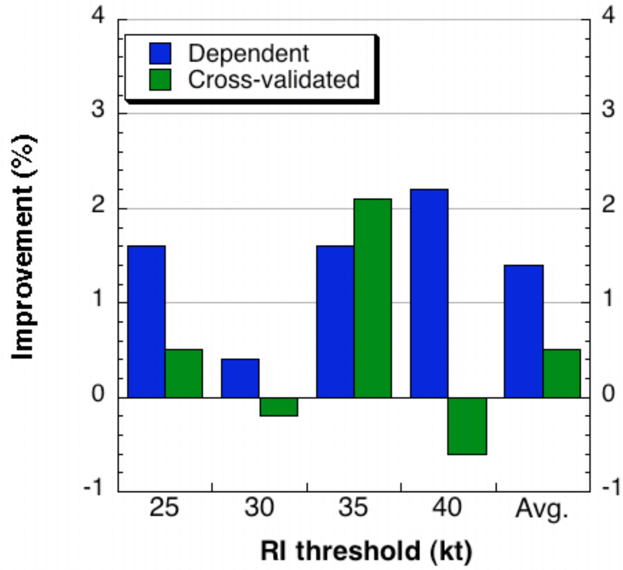

Fig. 5. Improvement in skill of the experimental RII obtained when ocean heat content was added as a 9th predictor to the Atlantic experimental RII. Results are shown for the dependent and cross-validated (independent) 1995-2008 samples for each individual RI threshold as well as for the average skill (Avg.) that was obtained for all 4 RI thresholds.

Atlantic RII in real-time. In addition, GOES-IR principle component analysis, TPW, and GFS boundary-layer predictors were generated for cases from the 2009 Atlantic hurricane season.

The updated 1995-2009 SHIPS developmental dataset that includes the aforementioned newly developed (TPW, GFS, GOES-IR PCs) predictors will be used to re-derive the experimental Atlantic RII for use during the upcoming 2010 Hurricane Season. In addition, a routine will be written to compute and output the new RII results in real-time. The experimental Atlantic RII will then be run in near real-time at CIRA and the output made available to the NHC commencing at the latter part of August 2010.

5. Development of E. Pacific RI predictors and derivation of experimental E. Pacific RII

Preliminary development of RI predictors for use in the derivation of an experimental E. Pacific RII has commenced. A total of 15 new boundary-layer predictors have been generated using GFS analyses for the 1995-2008 developmental sample. Also, the formatted TPW files required to generate the E. Pacific TPW predictors have been created for the 1995-2008 developmental sample. Finally, the generation of GOES-IR imagery for the Eastern Pacific 1996 season, which previously did not exist, has begun. The complete image records for TD01, TD02, Alma, Boris, Christina, Douglas, TD06, and Elida have been created and partial records for Genevieve have also been generated. These additional cases will be employed to increase the sample of E. Pacific cases that will be used when performing the principle component analysis on the GOES-IR imagery for that basin.

In year 2 of the proposal, new RI predictors for the E. Pacific basin will continue to be refined/developed using GFS, TPW, and GOES-IR data using the updated developmental database for the period from 1995-2009. These newly developed RII predictors will then be subjected to the same statistical screening tests that were utilized for the Atlantic basin and those found to provide the potential for increasing the skill of the existing RII will be used to derive a new experimental version of the E. Pacific RII. This new experimental E. Pacific RII will then be tested in real-time during the 2011 Hurricane Season.

6. Project timeline

August 2010 - Complete development of new inner-core predictors for E. Pacific RII
August 21 - November 30 2010- Perform near real-time tests of new experimental Atlantic RII
December 2010- Finalize revised experimental inner-core version of E. Pacific RII
March 2011 - Present year 2 results at IHC
June-November 2011- Perform real-time tests of experimental versions of Atlantic and E. Pacific RII
August 2011 – Provide final code for running experimental Atlantic and E. Pacific RII as part of SHIPS/LGEM operational guidance suite on IBM to TPC/NHC
August 1 2011- Year two ends final report due.

7. References

Cione, J.J., and E.W. Uhlhorn, 2003: Sea Surface temperature variability in hurricanes: Implications with respect to intensity change. *Mon. Wea. Rev.,* **131**, 1783-1796.

____, J. Kaplan, C Gentemann, and M. DeMaria, 2005. Developing an inner-core SST cooling algorithm for SHIPS. 8pp. [Available at http://www.nhc.noaa.gov/jht/03-05_proj.shtml].

Dunion, J.D., 2010: Re-writing the climatology of the tropical North Atlantic and Caribbean Sea atmosphere. J. Climate, *In press*.

Kaplan, J. , M. DeMaria, and J.A. Knaff, 2010: A revised tropical cyclone rapid intensification index for the Atlantic and Eastern North Pacific basins, *Wea. Forecasting*, **25**, 220-241.

Knaff, J.A., 2008: Rapid tropical cyclone transitions to major huricane intensity: Structural evolution of infrared imagery. *Preprints 28th Conf. on Hurricanes and Tropical Meteorology*, Orlando, FL, Amer. Meteor. Soc. .